# Article

# Asymmetric CLASP-Dependent Nucleation of Noncentrosomal Microtubules at the *trans*-Golgi Network

Andrey Efimov,[1,8] Alexey Kharitonov,[2,8] Nadia Efimova,[1] Jadranka Loncarek,[3] Paul M. Miller,[1]
Natalia Andreyeva,[2] Paul Gleeson,[4] Niels Galjart,[5] Ana R.R. Maia,[6] Ian X. McLeod,[7] John R. Yates, III,[7]
Helder Maiato,[6] Alexey Khodjakov,[3] Anna Akhmanova,[5] and Irina Kaverina[1,*]

[1] Department of Cell and Developmental Biology, Vanderbilt University Medical Center, Nashville, TN 37232, USA
[2] Institute of Molecular Biotechnology (IMBA), Austrian Academy of Sciences, Vienna A1030, Austria
[3] Wadsworth Center, New York State Department of Health, Albany, NY 12201, USA
[4] Department of Biochemistry and Molecular Biology and Bio21 Molecular Science and Biotechnology Institute,
The University of Melbourne, Melbourne, Victoria 3010, Australia
[5] Department of Cell Biology and Genetics, Erasmus MC, 3000 DR Rotterdam, The Netherlands
[6] Institute for Molecular and Cell Biology and Laboratory of Cell and Molecular Biology, Faculty of Medicine, University of Porto,
Porto 4050-345, Portugal
[7] Department of Cell Biology, Scripps Research Institute, La Jolla, CA 93037, USA
[8] These authors contributed equally to this manuscript.
*Correspondence: irina.kaverina@vanderbilt.edu
DOI 10.1016/j.devcel.2007.04.002

## SUMMARY

**Proper organization of microtubule arrays is essential for intracellular trafficking and cell motility. It is generally assumed that most if not all microtubules in vertebrate somatic cells are formed by the centrosome. Here we demonstrate that a large number of microtubules in untreated human cells originate from the Golgi apparatus in a centrosome-independent manner. Both centrosomal and Golgi-emanating microtubules need γ-tubulin for nucleation. Additionally, formation of microtubules at the Golgi requires CLASPs, microtubule-binding proteins that selectively coat noncentrosomal microtubule seeds. We show that CLASPs are recruited to the *trans*-Golgi network (TGN) at the Golgi periphery by the TGN protein GCC185. In sharp contrast to radial centrosomal arrays, microtubules nucleated at the peripheral Golgi compartment are preferentially oriented toward the leading edge in motile cells. We propose that Golgi-emanating microtubules contribute to the asymmetric microtubule networks in polarized cells and support diverse processes including post-Golgi transport to the cell front.**

## INTRODUCTION

Microtubules (MTs) serve as highways for intracellular transport arranging appropriate distribution of organelles and signals within a cell. Precise spatial and temporal reg-

ulation of MT distribution is essential for numerous cell functions.

In animal cells, centrosomes serve as the principal MT-organizing centers (MTOCs). Centrosomes organize symmetric MT arrays of uniform polarity, where MT minus ends are embedded in the centrosome while the highly dynamic plus ends extend toward the cell periphery. MT nucleation can also occur via centrosome-independent mechanisms. MT nucleation events have been described at the cell periphery far from the centrosome (Yvon and Wadsworth, 1997), and cells lacking centrosomes form relatively normal MT arrays (Khodjakov et al., 2000). A number of MT-organizing structures have been identified in interphase cells. Among these are the nuclear envelope in myotubes (Bugnard et al., 2005), plasma membrane of polarized epithelia (Reilein and Nelson, 2005), and melanosomes in pigment cells (Malikov et al., 2004). However, these sites appear to be functional only in specialized cell types. The question of where noncentrosomal MTs are nucleated in nondifferentiated cells remains open.

There have been reports that purified Golgi membranes support MT nucleation. In cells reforming MTs upon nocodazole washout, short MTs consistently associate with the Golgi (Chabin-Brion et al., 2001). This work suggested that the Golgi could serve as an MTOC. However, it remained ambiguous whether Golgi-associated MTs found in nocodazole washouts were in fact nucleated at the Golgi or whether they were nucleated by the centrosome but consequently released and captured by the Golgi (Rios et al., 2004). This latter scenario is probable, as MT minus ends are known to have affinity for Golgi membranes (Rios et al., 2004).

Indeed, it is very difficult to prove de novo MT nucleation at the Golgi. During interphase, the Golgi complex consists of membrane cisternae stacks with distinct polarity (Ladinsky et al., 2002) arranged in a complex
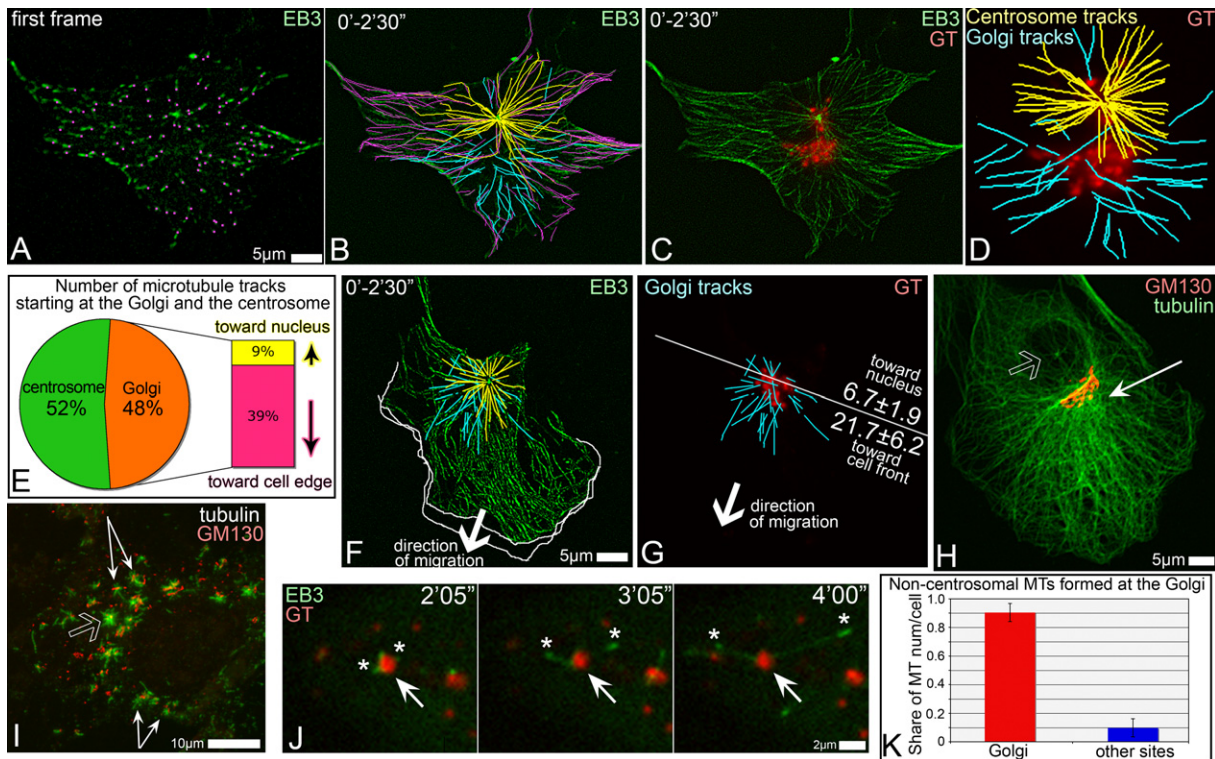
**Figure 1. The Golgi Complex Is an Additional MTOC**

(A–D) Detection of Golgi-originated MTs in time-lapse recording of GFP-EB3- and mCherry-GT-expressing RPE1 cells (5 s/frame). (A) GFP-EB3 in the first frame of the video (green). Currently growing MTs are marked by magenta dots. (B) Overlaid GFP-EB3 showing MT tracks within 2.5 min. Magenta, tracks started at the first frame. Yellow, centrosomal tracks; cyan, noncentrosomal tracks. (C) Overlaid GFP-EB3 (green) and mCherry-GT (red) images within 2.5 min. (D) Centrosomal (yellow) and noncentrosomal (cyan) MT tracks in the cell center and their relation to the Golgi position (GT, red).

(E) Percentage and directionality of Golgi-associated tracks (583 tracks in ten cells, analyzed as above).

(F and G) Directionality of Golgi-associated tracks in a motile cell. Arrows indicate the direction of the cell relocation. (F) Overlaid mCherry-EB3 tracks (2.5 min, false-colored green). Centrosomal (yellow) and Golgi-associated (cyan) tracks in the cell center are shown. Outlines of the protruding cell front in the first and last frames of the 5 min video are shown as white lines. (G) Golgi (YFP-GT, false-colored red) and associated tracks (cyan). A line is drawn perpendicular to the direction of cell movement. The average numbers of MTs in nine cells growing forward or backward are shown.

(H) A prominent MT array (thin arrow) in a polarized cell is associated with the Golgi (red) rather than with the centrosome (hollow arrow). Tubulin, green; GM130, red; immunostaining.

(I) RPE1 cell fixed and stained 45 s after nocodazole washout. MTs (green) radiate from the Golgi mini-stacks (thin arrows) and the centrosome (hollow arrow). Tubulin, green; GM130, red.

(J) Live-cell images of nocodazole washout. GFP-EB3-rich plus tips (green, asterisks) grow away from the mCherry-GT-marked Golgi stack (arrow, red).

(K) Number of noncentrosomal MTs nucleated at the Golgi (red) and elsewhere (blue) after nocodazole washout per cell, based on live recordings of mCherry-EB3- and YFP-GT-expressing cells (521 MTs in eight cells). Error bars indicate standard deviations.

"ribbon" situated very close to the centrosome. For this reason, Golgi-associated MT arrays could be easily confused with those originating from the centrosome. We have overcome this difficulty by developing a technique that allows us to trace individual MTs back to their point of origin in live cells. This approach reveals that the Golgi nucleates MTs under physiological conditions. In sharp contrast to the centrosome, MT arrays organized by the Golgi are inherently asymmetric.

Our data demonstrate that MT nucleation at the Golgi requires the MT +TIP proteins CLASPs, which have been previously localized to the Golgi (Akhmanova et al., 2001). Here we provide evidence that CLASPs associate specifically with the *trans*-Golgi network (TGN) protein GCC185. Thus, CLASPs concentrate only in the TGN,

leading to the asymmetry of the MT array nucleated at the Golgi.

## RESULTS

### Identification of MT Nucleation Sites in Interphase Cells

MT nucleation at centrosomes was previously analyzed by tracking fluorescently labeled plus tip-binding protein (Piehl et al., 2004). We have adopted this approach to detect the origin of noncentrosomal MTs in retinal pigment epithelial (RPE1) cells (Figures 1A–1D) during interphase. MT tips were visualized by fluorescently labeled EB3 (Figure 1) or CLIP170 (see Figure S1 in the Supplemental Data available with this article online). MTs that carried EB3

signal in the first frame of the video sequence had been nucleated before we initiated our observations, and thus their origin could not be determined (Figure 1A). Such MT tracks (Figure 1B, magenta) were excluded from further analysis. All MT tracks that were initiated during the recording were divided into two distinct groups. First, MTs that originated from a common perinuclear site (~2 μm in diameter) were regarded as centrosomal. These MTs consistently formed a radial symmetric array (Figures 1B, 1D, and 1F, yellow). Parallel analysis of similarly obtained EB3 tracks in cells coexpressing GFP-centrin revealed that the centrosome was always in the middle of these radial arrays (data not shown). The second group of MTs originated from a larger common area spatially separated from the centrosome (Figure 1B, cyan). In addition to these two major groups, a few MT tracks emerged close to the cell periphery. These tracks likely corresponded to MTs that were not truly nucleated during our observations but rather rescued as the result of dynamic instability. It is important to emphasize that whereas MT rescues are relatively frequent in the peripheral parts of the cytoplasm, they are extremely rare in the center of the cell (Komarova et al., 2002; unpublished data). Thus, most of those tracks that originate near the cell center represent outgrowth of newly nucleated MTs.

### Noncentrosomal MTs Are Nucleated at the Golgi Complex

The fact that most of the noncentrosomal MTs originated from a discrete site suggested that they are nucleated by a common mechanism. Overlaying the tracks of noncentrosomal MTs with the Golgi marker GT (membrane-binding domain of galactosyl transferase) revealed that the noncentrosomal MTs grew from the Golgi (Figures 1C and 1D). This was particularly obvious in cells where the centrosome and the Golgi were spatially separated. The number of MTs originating from the Golgi was slightly lower than those nucleated at the centrosome (22.5 ± 3.2 versus 30.5 ± 5.5 per cell in 2.5 min).

MT nucleation at the centrosome resulted in symmetrical arrays, consistent with previous findings (Salaycik et al., 2005). In contrast, MTs growing from the Golgi (Figure 1E) were biased toward the cell edge (away from the nucleus). In motile cells (Figures 1F and 1G), where the Golgi complex is oriented to the leading cell edge, Golgi-originated MTs were preferentially directed toward the cell front, likely contributing to a directional MT array (Figure 1H) that is considered important for motile cell polarization.

To further clarify the nature of MT nucleation sites in spread cells, we depolymerized MTs with nocodazole and then followed the MT repolymerization pattern. Tubulin stainings after short periods of regrowth revealed numerous noncentrosomal MTs along with the radial centrosomal array (Figure 1I; Figure S2). The Golgi complex in the absence of MTs was dispersed to mini-stacks spread throughout the cytoplasm. The majority of noncentrosomal MTs was found attached to the mini-stacks, consistent with previous reports (Chabin-Brion et al., 2001).

Time-lapse imaging of cells expressing 3GFP-EMTB or GFP-EB3 together with mCherry-GT revealed that noncentrosomal MTs were directly initiated at Golgi membranes (Figure 1J). Statistical analysis confirmed that the loci of the first appearance of detectable EB3 dots colocalized with the Golgi stacks (Figure 1K). MTs in these experiments were detected at the Golgi and the centrosome simultaneously. Recordings of EB3-marked MT plus ends revealed that the plus ends polymerized away from the Golgi stacks, while the minus ends stayed attached to the Golgi (Figure 1J). These results support the conclusion that the Golgi microenvironment is necessary for successful noncentrosomal MT formation.

### MT Nucleation at the Golgi Is Centrosome Independent but Requires γ-Tubulin

The fact that MTs appear simultaneously in different parts of the cytoplasm during recovery from nocodazole treatment argues strongly that Golgi-associated MTs form at the Golgi independently of the centrosome. However, in the steady state, the Golgi and the centrosome are in close proximity and thus it is formally possible that MTs formed at the centrosome can be released and anchored to the Golgi membranes. In order to unequivocally test whether the Golgi functions as an MTOC, we selectively destroyed GFP-centrin-labeled centrosomes by the laser microsurgery technique (Figures 2A–2L). It has been demonstrated that this approach results in complete disappearance of MTs directly associated with the centrosome in a matter of minutes (Khodjakov et al., 2000). However, overall organization of cells lacking centrosomes resembles that of centrosomal cells (Khodjakov and Rieder, 2001). MT-tracking analyses conducted at least 30 min after centrosome ablation revealed that radial arrays of MTs normally growing from the centrosome were absent in cells lacking the centrosome (Figures 2A–2L). In contrast, MTs continued to grow persistently from the Golgi complex, revealing that this organelle can function as an MTOC even in the absence of centrosomes.

MT nucleation at the centrosome requires molecular templates known as γ-tubulin-ring complexes (γ-TuRC). Previous studies suggested that γ-tubulin may also be associated with the Golgi membranes (Chabin-Brion et al., 2001; Rios et al., 2004). In order to test directly whether MT nucleation at the Golgi requires γ-TuRC, we depleted γ-tubulin from RPE1 cells by siRNA (Figure 2M). The number of newly nucleated noncentrosomal MTs in nocodazole washout experiments depended on the amount of γ-tubulin in the cytoplasm (Figures 2N–2R). Thus, similar to the centrosome, MT nucleation at the Golgi requires γ-TuRC.

### MT Regulators CLASPs Localize at the TGN via Association with TGN Protein GCC185

To identify molecular players involved in MT formation at the Golgi, we investigated the plus end-binding proteins CLASPs, which are potent regulators of MT dynamics. CLASPs were previously detected at the centrosome
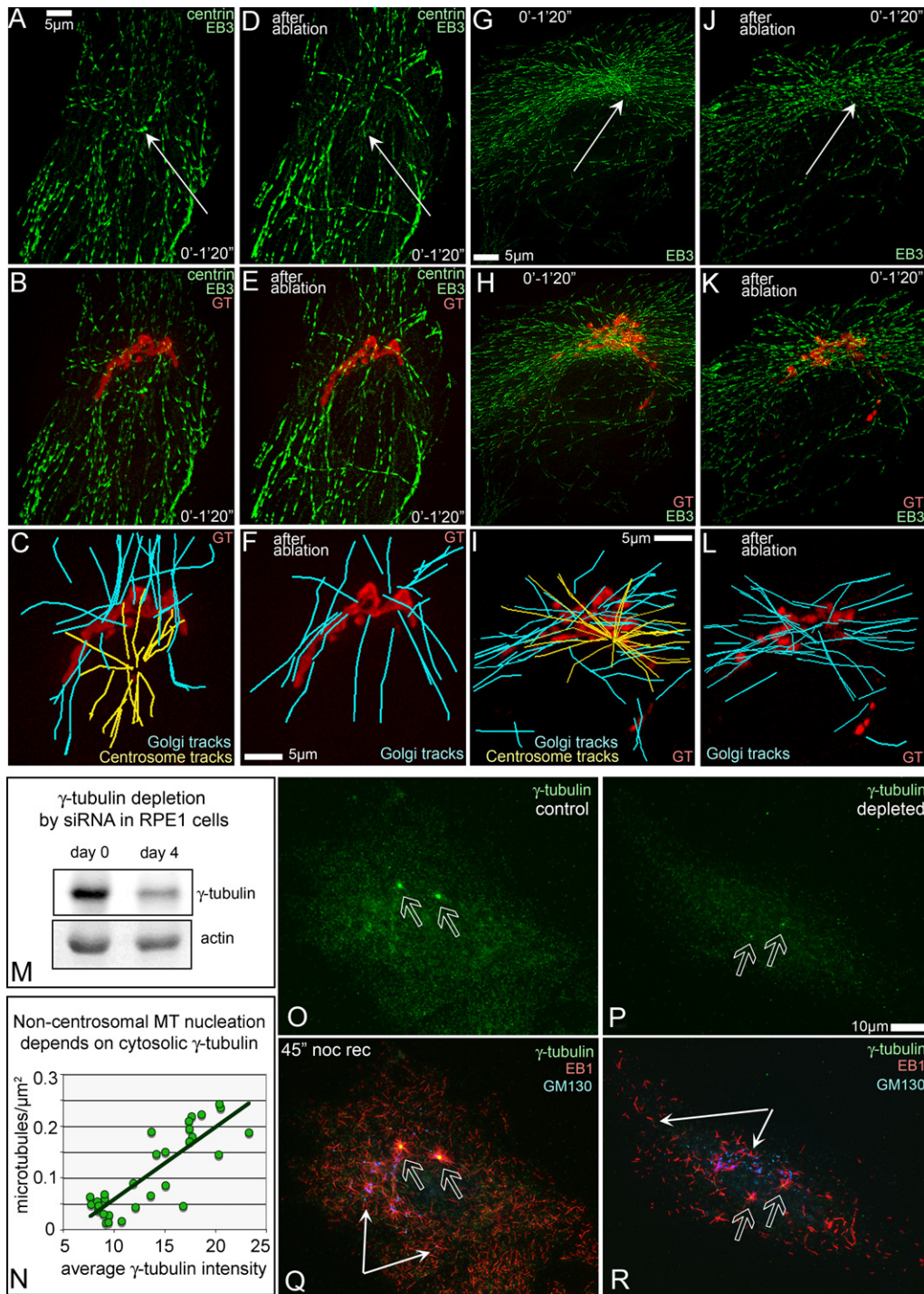
**Figure 2. MT Nucleation at the Golgi Does Not Require the Centrosome but Needs γ-Tubulin**

(A–L) (A–F) GFP-EB3- (green), GFP-centrin- (green), and mCherry-GT- (red) expressing cells. (G–L) GFP-EB3- (green) and mCherry-GT- (red) expressing cells. (A–C and G–I) Cells prior to ablation. (D–F and J–L) Cells 30 min after ablation. Nucleation sites were analyzed as in Figures 1A–1D. (A, D, G, and J) EB3 tracks within 1 min 20 s. Arrows, centrosomes. (B, E, H, and K) EB3 tracks (green) superimposed on the Golgi image (GT, red). (C, F, I, and L) Centrosomal (yellow) and noncentrosomal (cyan) MT tracks in the cell center and their relation to the Golgi position (GT, red). Centrosomal but not Golgi-originated arrays disappear after centrosome ablation (F and L).

(M) Fifty percent depletion of γ-tubulin in RPE1 cells by siRNA. Actin, loading control.

(N) Number of noncentrosomal MTs directly corresponds to intensity of cytosolic γ-tubulin staining.

(O–R) Fewer centrosomal (hollow arrows) and noncentrosomal (thin arrows) MTs are formed 45 s after nocodazole washout in γ-tubulin-depleted (P and R) than in control (O and Q) cells. γ-tubulin, green (O–R); EB1, red (Q and R); GM130, blue (Q and R); immunostaining.

and the Golgi (Akhmanova et al., 2001). In mammalian cells, CLASPs exist as two closely related homologs, CLASP1 and CLASP2. In all experiments described below, we visualized both of them using either a mixture of CLASP1 and CLASP2 antibodies or a pan-CLASP antibody (VU-83; Figure S3).

CLASPs are localized to MT tips, the centrosome, and the Golgi. By costaining for CLASPs and Golgi compartment markers, we have found that CLASPs specifically colocalize with the TGN marker TGN46 (Figures 3A and 3B) but not with *cis*- and *mid/trans*-Golgi markers (Figure S4). This indicates that CLASPs specifically bind the outer subcompartment of the *trans*-Golgi, TGN, and are absent from other Golgi compartments.

In detergent extraction experiments, CLASPs behave as peripheral membrane proteins (Figure S5). To search for Golgi components that recruit CLASPs to the Golgi membranes, we used HeLa cells stably expressing LAP-tagged GFP-CLASP1α. Coimmunoprecipitation with anti-GFP antibodies and subsequent mass spectrometry analysis revealed the GRIP-domain-containing protein GCC185 (Luke et al., 2003) as a part of a complex together with known CLASPs-interacting partners (Table S1). Further, endogenous CLASP2 specifically coprecipitated with ectopically expressed myc-tagged GCC185 from HEK293T cells by either anti-CLASP or anti-myc antibodies (Figure 3C). This indicates that either CLASP isoform is able to bind GCC185.

GCC185 is a peripheral membrane protein specifically distributed to the TGN. In RPE1 cells, GCC185 shows significant colocalization with CLASPs at the Golgi in untreated (Figures 3D–3H) as well as in nocodazole-treated cells, where the Golgi ribbon is dispersed into individual mini-stacks (Figures 3I–3L).

To gain further support for the interaction of CLASPs and GCC185, we took advantage of the CLASP mislocalization approach. We produced an expression construct that contains dTOM20 (*Drosophila* outer mitochondrial protein) fused to CLASP2. Chimeric mito-CLASP localized specifically to the mitochondria when ectopically expressed in RPE1 cells (Figure 3M). It was recognized by anti-CLASP antibodies in immunofluorescence (Figure 3M) and western blotting and sequestered known CLASP partners CLIP170, CLIP115, and EB1 to the mitochondria (data not shown). Importantly, GCC185 was readily recruited to mistargeted mitochondria-bound CLASP2, whereas normally it does not localize to mitochondria (Figures 3N–3R).

As a membrane-associated GRIP-domain golgin, GCC185 may serve as a scaffolding protein for CLASPs at the TGN. To evaluate this possibility, we depleted GCC185 from RPE1 cells by siRNA, resulting in up to 90% protein loss (Figure 3S). Loss of GCC185 led to exclusion of CLASPs from the TGN, whereas MT plus end-associated CLASPs remained uninfluenced (Figures 3T–3V). Expression of a nonsilenceable GCC185 variant rescued the phenotype (Figures S6A and S6B).

Together, these results demonstrate that GCC185 recruits CLASP to the TGN that is located at the convex side of Golgi stacks. Thus, CLASPs are plausible candidates for facilitating MT assembly at this location.

## CLASP Depletion from RPE1 Cells Impairs MT Formation at the Golgi and Alters MT Pattern

Because the major known function of CLASPs is regulation of MT dynamics, we tested whether Golgi-associated CLASPs are involved in MT-organizing activity at the Golgi.

We depleted up to 75% of both CLASP1 and CLASP2 proteins from RPE1 cells as described (Mimori-Kiyosue et al., 2005) (Figure 4A). Localization of CLASP-binding proteins EB1 and CLIP170 to MT plus ends was not impaired by CLASP knockdown (Figure S7).

Nocodazole washout experiments in mixed cultures of CLASP-positive and CLASP-depleted cells revealed a striking difference in the formation of noncentrosomal MTs (Figures 4B–4F). In CLASP-positive cells, numerous noncentrosomal MTs radiated from Golgi mini-stacks (Figure 4C). In contrast, CLASP-depleted cells contained much lower numbers of noncentrosomal MTs not associated with Golgi mini-stacks (Figure 4D). Ectopic expression of GFP-CLASP2 in CLASP-depleted cells rescued the phenotype to control levels of noncentrosomal nucleation (Figure 4B; Figures S6G–S6J). Live-cell imaging of MT recovery in CLASP-depleted cells confirmed elimination of Golgi-initiated MT outgrowth (Figures 4G and 4H).

In order to determine whether CLASP-dependent MT formation affects interphase MT networks, we used the plus tip tracking approach illustrated in Figures 1A–1D. Upon CLASP depletion, centrosomal MT nucleation was not altered but the number of MTs growing from the Golgi decreased dramatically (Figures 5A–5C, 5G, and 5H). Similarly, the number of Golgi-emanating MTs was significantly lowered in GCC185-depleted cells that lack CLASP at the Golgi (Figures 5D–5H). Further, we directly compared MT patterns in control, CLASP-depleted, and GCC185-depleted cells immunostained for tubulin. Cells depleted of either CLASPs (Figures 5I and 5J) or GCC185 (Figures 5K and 5L) lacked the dense meshwork of MTs characteristic of the Golgi area, as well as the extensive MT array directed to the leading cell edge.

These data suggest a specific role for CLASPs at the TGN in the formation of Golgi-associated MTs. In contrast, centrosomal MTs were not affected by CLASP or GCC185 depletion.

## Noncentrosomal MT Seeds Are Coated with CLASPs and Anchored to the Golgi Membrane

Our results suggest that CLASPs are required for MT formation at the Golgi but not at the centrosome. Consistent with this idea, immunostaining of steady-state MTs revealed that the amount of CLASP associated with MT tips was significantly higher for MTs growing from the Golgi than for those growing from the centrosome (Figures 6A and 6B). Moreover, live-cell imaging showed that GFP-CLASP2-highlighted MTs originated at CLASP-containing TGN membranes (Figure 6C) but not at the centrosome. At the initial stages of MT outgrowth at the Golgi,
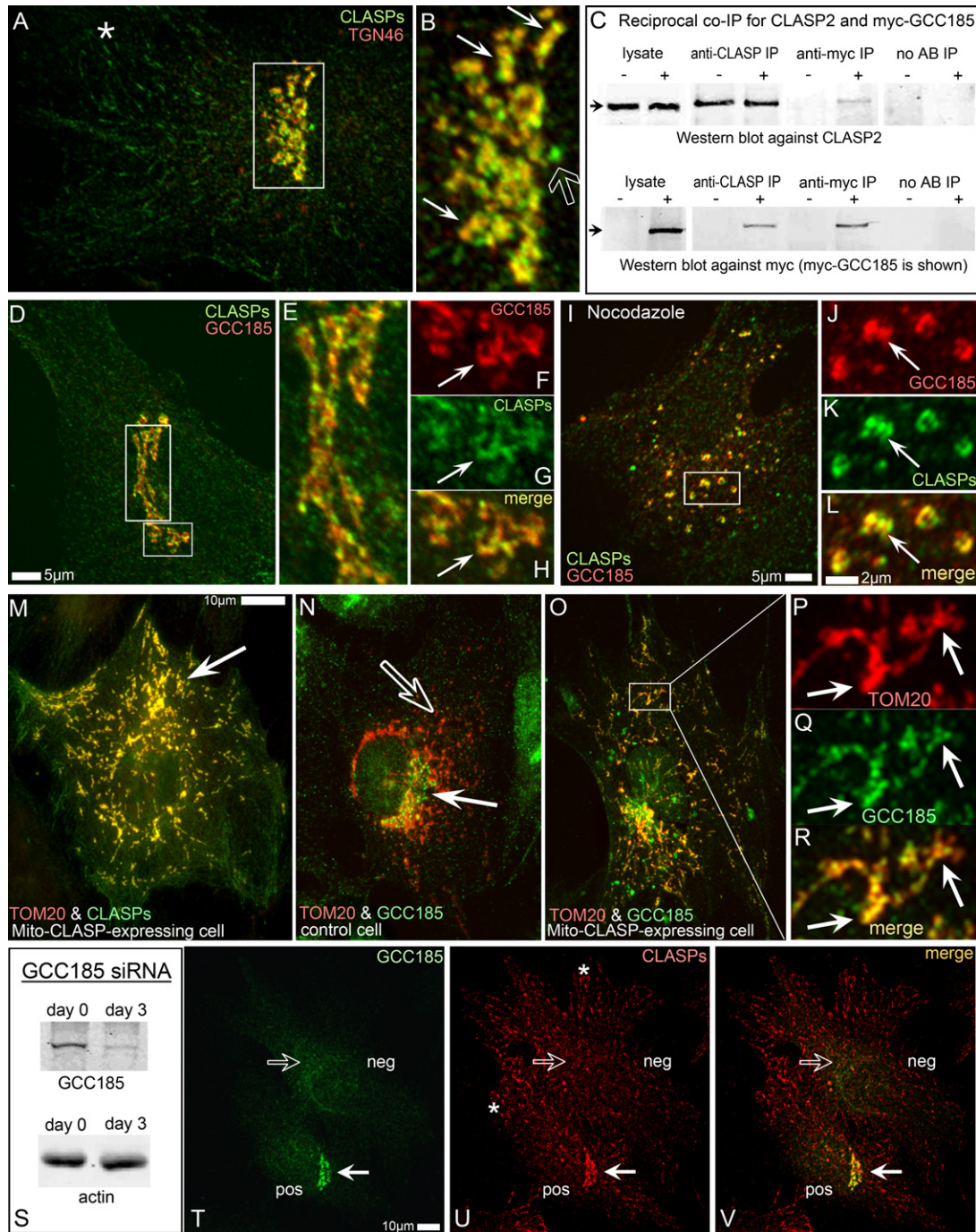
**Figure 3. CLASPs Specifically Localize to TGN Membranes via GCC185 Binding**

(A and B) CLASPs (green) colocalize with TGN46 (red, thin arrows in [B]) along with the MT tips (star in [A]) and the centrosome (hollow arrow in [B]). Box in (A) is enlarged in (B).

(C) Coimmunoprecipitation of CLASP2 and myc-GCC185 using either anti-CLASP2 or anti-myc antibodies. Upper panel, CLASP2; lower panel, myc-GCC185. Nontransfected cells are marked as "−," myc-GCC185-transfected cells as "+." CLASP2 is coprecipitated from transfected cells by anti-myc antibody (anti-myc IP). Myc-GCC185 is coprecipitated from transfected cells by anti-CLASP antibody (anti-CLASP IP). Antibody-free beads are used as control (no AB IP).

(D–H) CLASP colocalizes with ectopically expressed myc-tagged GCC185 at the TGN. Myc, red; CLASP, green. (E) Enlarged tall box from (D). (F–H) Enlarged small box from (D). (F) Myc-GCC185. (G) CLASP. (H) Merge. Arrows, reference point.

(I–L) Association of CLASPs and GCC185 is preserved in nocodazole. (J–L) Enlarged small box from (I). (J) Myc-GCC185. (K) CLASPs. (L) Merge. Arrow, reference point.

GFP-CLASP2 was distributed along the entire MT length (up to 2 μm; Figure 6D). At later stages, CLASP2 remained associated with the TGN and with the growing plus end (Figure 6D, 40 s). Fixed-cell (Figures 6E–6G) or live-cell (Figures 6I–6K) nocodazole washout assays confirmed that noncentrosomal MTs were completely coated with CLASPs at early stages of regrowth. In contrast, only a moderate amount of CLASPs could be detected at MTs growing from the centrosome. CLASP-binding MT tip proteins EB1 and CLIP170 did not display differential association with Golgi-associated versus centrosomal MTs (Figure 6B; Figure S7).

Initial coating of Golgi-originated MTs by CLASPs suggests that CLASPs may be directly redistributed to MT seeds from the Golgi membrane and stabilize them. If this hypothesis is true, CLASPs should be able to nucleate microtubules even when they are not associated with the Golgi. To test this prediction, we analyzed MT regrowth after nocodazole washout in cells where CLASPs were displaced from the TGN by GCC185 depletion (Figures 3T–3V). The number of noncentrosomal MTs formed after nocodazole removal did not significantly differ from controls (Figures 7A–7D and 7I), indicating that CLASPs can support MT formation also when they are not bound to the Golgi membranes. Similarly, MT numbers after nocodazole washout were not altered by brefeldin A (BFA) treatment (Figure 7I), which causes dissociation of CLASPs (Figure 7E) as well as other peripheral Golgi proteins (Presley et al., 1998) from the membrane. Persistence in noncentrosomal MT formation may be due to the fact that CLASP binding to MT tips as well as CLASP coating of MT seeds upon nocodazole washout were not affected by either BFA treatment (Figures 7F–7H) or GCC185 depletion (data not shown). Additional depletion of CLASPs resulted in elimination of noncentrosomal nucleation under those conditions (Figure S8).

We also investigated whether noncentrosomal MTs were formed at particular nucleation sites when CLASPs were dissociated from the Golgi membranes. Therefore, we registered all loci where noncentrosomal MTs were first detected in nocodazole washout experiments. Unlike controls (Figure 7J, red; Figure 7K), noncentrosomal MTs formed in the presence of BFA did not arise from distinct centers. Instead, single MTs were randomly distributed in the cytoplasm (Figure 7J, green; Figure 7L), similar to those in GCC185-depleted cells (Figures 7A–7D; Figures S6C–S6F).

Live-cell video analyses revealed that after noncentrosomal MTs were formed, instead of elongating with their minus ends anchored at the sites of nucleation, short MT fragments relocated in the cytoplasm, most likely due to treadmilling (Figure 7L).

These data indicate that while CLASPs can support MT nucleation both at the Golgi and in the cytosol, their association with the Golgi membrane is needed for anchoring and stabilization of the minus ends of noncentrosomal MTs.

## DISCUSSION

Our results reveal that CLASPs are critical players in the noncentrosomal MT nucleation at the TGN membranes. As MTs can form in the cytoplasm of GCC185-depleted or BFA-treated cells, we conclude that CLASPs are necessary for MT formation whereas membrane binding is not. MTs probably preferably form at the TGN due to high concentration of CLASP molecules at this location. Because γ-tubulin is likely needed for nucleation per se, we suggest that CLASPs selectively stabilize preexisting MT seeds. It has been suggested before (Lansbergen et al., 2006) that CLASPs accumulated in the proximity of the plasma membrane can stabilize MTs without capping their plus ends. Such stabilization is likely due to the ability of CLASPs to bind the MT lattice (Wittmann and Waterman-Storer, 2005). We propose that a similar mechanism assures selective survival of MT seeds at the TGN membranes (see model in Figure 7M). Being MT tip-binding proteins, CLASPs have a high affinity for newly polymerized MT regions including freshly nucleated MT seeds. Prominent localization to the Golgi indicates that CLASPs also have a high affinity for Golgi membranes. We suggest that CLASPs at the Golgi membranes are able to anchor very short MT fragments formed in their proximity, and by coating them prevent their disassembly and allow them to serve as seeds for polymerization. This model suggests that redistribution of CLASP molecules from the Golgi to growing MTs is critical for CLASP function. Consistent with our model, the mito-CLASP chimera that is irreversibly bound to mitochondrial membranes exhibited no potential for MT nucleation (data not shown). As MTs elongate, CLASPs remain associated with the structures for which they have high affinity: plus ends and the Golgi membrane.

Interestingly, centrosomal MTs that do not depend on CLASPs are also not coated by CLASPs as they form. Such a deficiency may be due to selective GSK3β activation at the centrosome (Higginbotham et al., 2006) that can inhibit CLASP binding to the MT lattice (Akhmanova et al.,

(M) CLASP2-dTOM20 chimera (mito-CLASP) and mCherry-dTOM20- (red) coexpressing cell. CLASP staining (green) reveals both mito-CLASP (arrow; colocalized with mCherry-dTOM20 at mitochondria) and endogenous CLASPs.
(N) GCC185 at the Golgi (green, white arrow) does not colocalize with mCherry-dTOM20 at mitochondria (red, hollow arrow) in control cells.
(O–R) Mito-CLASP-expressing cell. Endogenous GCC185 (green) is recruited to mitochondria (mCherry-dTOM20, red). Box is enlarged in (P)–(R).
(P) mCherry-dTOM20. (Q) GCC185. (R) Merge. Arrows, reference points.
(S) GCC185 is 90% depleted from RPE1 cells by siRNA.
(T–V) Mixed culture of GCC185-depleted (neg) and control (pos) cells. (T) GCC185. (U) CLASPs. (V) Merge of (T) and (U). CLASP is localized to the Golgi in control cells (white arrow) but not in GCC185-depleted cells (hollow arrow). MT tip colocalization of CLASP is intact in both cells (asterisks). All images show immunostainings.
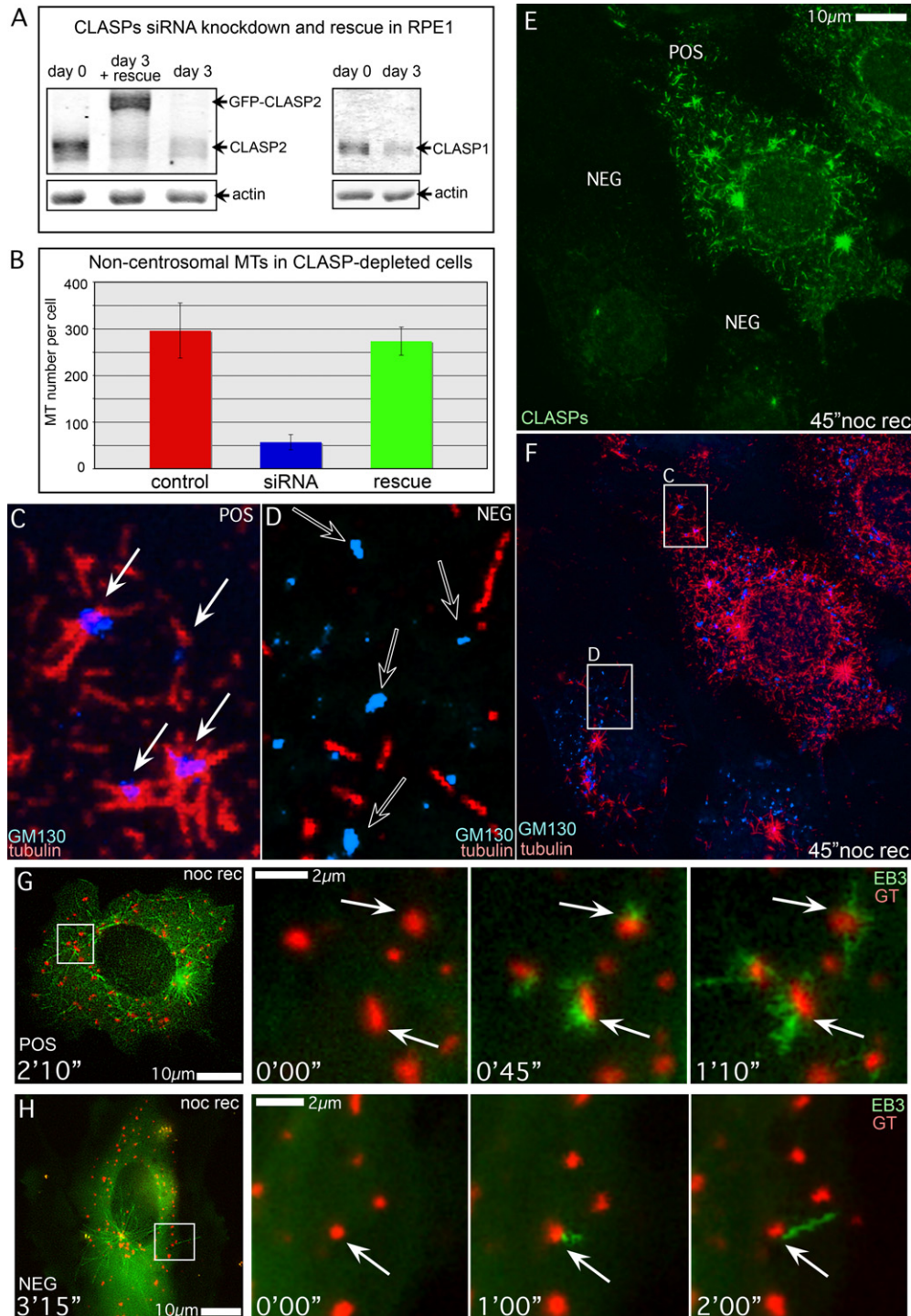
**Figure 4. siRNA CLASP Knockdown Suppresses MT Formation at the Golgi upon Nocodazole Washout**

(A) Western blotting illustrating ∼75% decrease in both CLASP1 and CLASP2 on the third day after siRNA transfection as well as expression of nonsilenceable GFP-CLASP2. Regions of interest are shown.

(B) Numbers of noncentrosomal MTs formed 45 s after nocodazole washout in CLASP-positive (red, 30 cells) and CLASP-depleted cells (blue, 30 cells), as well as upon rescue by nonsilenceable GFP-CLASP2 (green, 16 cells). Based on tubulin immunostaining. Error bars indicate standard deviations.

(C–F) Mixed culture of CLASP-positive (pos) and CLASP-depleted (neg) cells 45 s after nocodazole washout. Tubulin, red; GM130, blue; CLASPs, green; immunostaining. (C) In CLASP-positive cells, MTs radiate from Golgi stacks (arrows). (D) In CLASP-depleted cells, Golgi stacks are not associated with rare MTs (hollow arrows). (E and F) CLASPs (E) and MTs and Golgi stacks (F) at low magnification. Boxes are enlarged in (C) and (D).

2001; Wittmann and Waterman-Storer, 2005). The difference in CLASP binding to centrosomal and Golgi-associated MTs prompts us to speculate that these two groups of MTs may have different dynamic properties from the start. It is noteworthy in this regard that Golgi-associated MTs are acetylated more rapidly than centrosomal ones (Chabin-Brion et al., 2001), pointing to their elevated stability.

Understanding that CLASPs stabilize preexisting MT seeds leaves the question of where these seeds are formed unanswered. It is possible that high concentration of the seeds at the Golgi is established by recruitment of γ-TuRC to *cis*-Golgi proteins GMAP210 (Rios et al., 2004) or AKAP350 (Shanks et al., 2002). However, successful growth of these seeds is likely achieved only when they become associated with CLASP-rich TGN membranes. Thus, seeds may be formed at the *cis*-Golgi membranes, dissociate and bind TGN, or, consistent with the cisternal maturation model (Mironov et al., 2005), stay associated with maturing cisternae until they become enriched in TGN proteins, including GCC185 and CLASPs, which then promote MT growth.

Although not needed for the initiation of MT growth, the TGN membrane appears to serve as an anchoring site for noncentrosomal MT minus ends, thereby preventing them from depolymerization. The anchoring may involve yet unidentified molecular players. Alternatively, CLASPs bound to the membrane may accomplish the anchoring either by lateral MT binding or due to a yet unknown ability of CLASPs to cap MT minus ends. Actually, CLASPs are strongly associated with both minus end anchoring sites: the Golgi and the centrosome. In our experiments, anchoring and release of centrosomal MTs were not altered by CLASP depletion (data not shown). We have to admit, though, that siRNA knockdowns were not efficient enough to fully deplete CLASPs from the centrosome. Thus, the centrosome appears to have very strong affinity for CLASPs, suggesting that they may bear an important function at this location, possibly in minus end anchoring.

A striking feature distinguishing Golgi-associated arrays from centrosomal ones is their asymmetry. We suggest that this asymmetry is due to the selective MT formation only at CLASP-containing TGN membranes and not other Golgi compartments. Being asymmetric, Golgi-originated MT arrays could contribute to cell polarization.

The centrosome localization in front of the nucleus typical for many motile cells is thought to be an important stage in establishing MT asymmetry and, in turn, cell polarization (Raftopoulou and Hall, 2004). The centrosome itself nucleates symmetrically (Bergen et al., 1980; Salaycik et al., 2005). However, dynein-driven transport organizes an asymmetric MTOC, the Golgi, in close proximity to the centrosome. We suggest that centrosome localization influences MT asymmetry indirectly via the positioning of the Golgi complex. This model can explain such recent

data as direct correlation between MTOC (centrosome) positioning and formation of asymmetric MT arrays in neurons (de Anda et al., 2005).

Notably, CLASP2 was recently found necessary for persistent directional cell migration (Drabek et al., 2006). As Golgi-associated MT arrays in motile cells are oriented toward the cell front (see model in Figure 7N), they can be a source for pioneer MTs that are implicated in stabilization of protrusion and are important for the directionality of migration (Suter et al., 2004; Waterman-Storer et al., 1999). Additionally, Golgi-originated MTs in motile cells could facilitate turnover of adhesions behind the leading edge (Rid et al., 2005).

Importantly, Golgi-associated MTs could be involved in vesicular transport to, within, or out of Golgi stacks. As Golgi-originated MTs in motile cells directly connect the TGN with the cell front (Figure 7N), they may support vesicular transport toward the leading edge that is important to maintain high motility rates (Preisinger et al., 2004; Prigozhina and Waterman-Storer, 2004). In polarized epithelial cells, Golgi-dependent nucleation could originate vertical MT arrays that are associated with the Golgi at their minus ends and are responsible for baso-apical vesicular transport (Bacallao et al., 1989; Musch, 2004).

Overall, a CLASP-dependent mechanism of noncentrosomal MT formation at the Golgi could be engaged in various cell types where MTs not attached to centrosomes bear diverse functions (Bartolini and Gundersen, 2006).

## EXPERIMENTAL PROCEDURES

### Cells

Immortalized human pigment epithelial cells hTert-RPE1 (Clontech) were maintained in DMEM/F12, and HeLa, MDCK, RIE, BT549, and HEK293T cells in DMEM, all with 10% fetal bovine serum (FBS) at 37°C in 5% CO$_2$. IMCE cells were maintained in RPMI with 5% FBS and 1% insulin at 33°C. Cells were plated on fibronectin-coated glass coverslips 24 hr prior to experiments. Mixed cultures of control and knockdown cells were obtained by mixing trypsinized cell suspensions in a proportion of 1:1 before plating.

### Treatments

For MT depolymerization, nocodazole (2.5 μg/ml) was added to culture media for 2 hr. For nocodazole washout fixations, cells were rinsed five times with ice-cold medium and then moved to a dish with warm (37°C) medium (time 0 for MT regrowth). For live imaging of MT regrowth, cells were washed with cold medium directly at the microscope stage after initial recording of cells in nocodazole. Temperature was thus slowly raised by the heated stage. Slightly variable times of MT regrowth initiation in video sequences are due to this experimental setup.

BFA (Alexis Biochemicals) was used at 5 μg/ml in culture media. For nocodazole washout experiments of BFA-treated cells, nocodazole-containing and final wash nocodazole-free media were supplemented with BFA.

### siRNA and Expression Constructs

Mixed siRNA oligos against CLASP1 and CLASP2 (Mimori-Kiyosue et al., 2005) were transfected using Oligofectamine (Invitrogen) according to the manufacturer's protocol. Experiments were conducted

---

(G and H) Video frames illustrating MT formation at the Golgi (arrows) in mRFP-EB3 (false-colored green) and YFP-GT (false-colored red) in nocodazole washout. Time after nocodazole removal is shown. Left, frames showing whole cell. Areas in boxes are enlarged to the right. (G) Control cell. (H) CLASP-depleted cell.
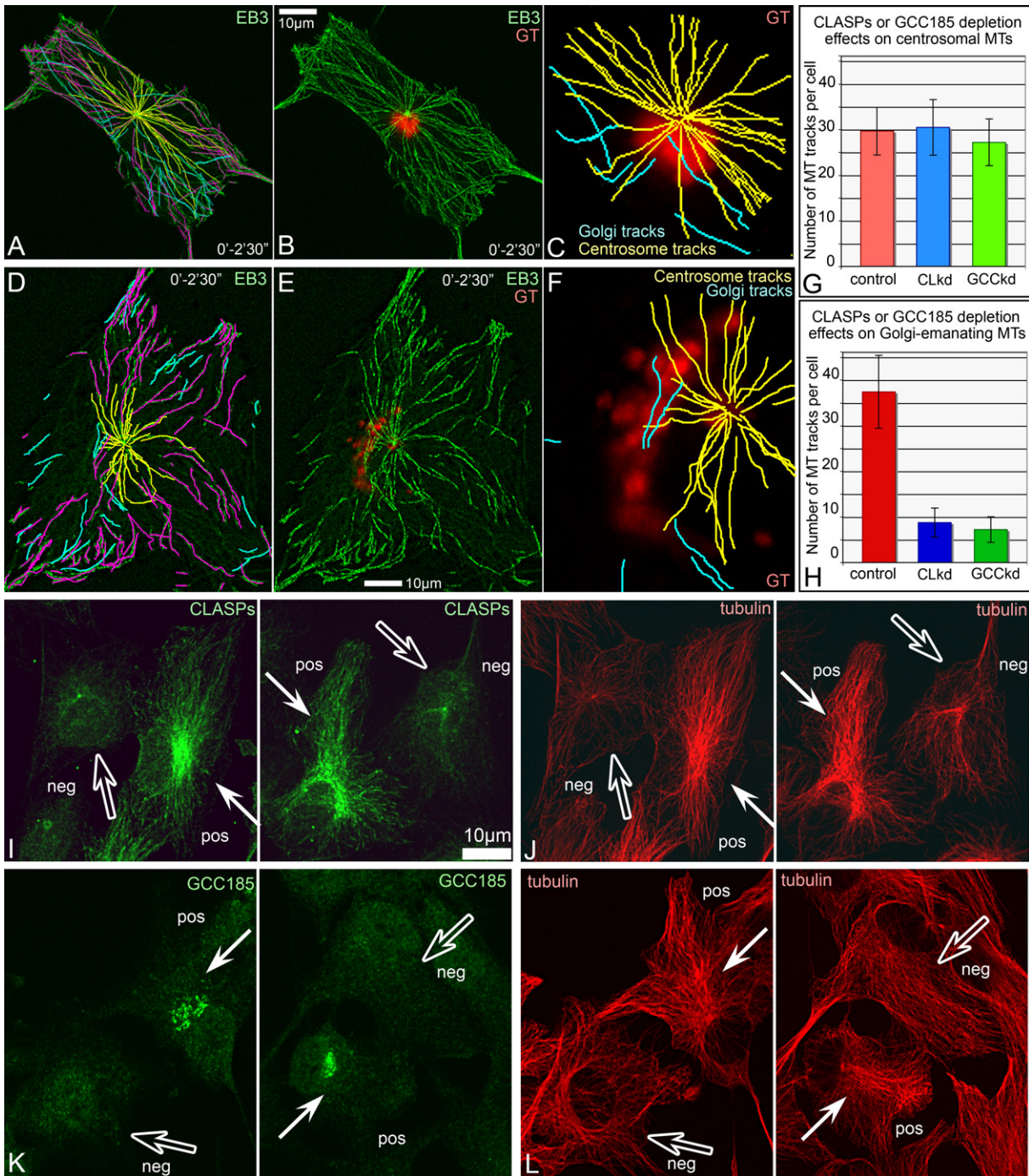
**Figure 5. Golgi-Originated MTs in Steady State Require CLASP Presence at the TGN**

(A–C) GFP-EB3- and mCherry-GT-expressing CLASP-depleted cells analyzed as in Figures 1A–1D. (A) Overlaid GFP-EB3 showing MT tracks within 2.5 min. Magenta, tracks started at the first frame. Yellow, centrosomal tracks; cyan, noncentrosomal tracks. (B) Overlaid GFP-EB3 (green) and mCherry-GT images within 2.5 min. (C) Centrosomal (yellow) and a few noncentrosomal (cyan) tracks in the cell center and their relation to the Golgi position.

(D–F) GFP-EB3- and mCherry-GT-expressing GCC185-depleted cells analyzed as in Figures 1A–1D. (D) Overlaid GFP-EB3 showing MT tracks within 2.5 min. Magenta, tracks started at the first frame. Yellow, centrosomal tracks; cyan, noncentrosomal tracks. (E) Overlaid GFP-EB3 (green) and mCherry-GT images within 2.5 min. (F) Centrosomal (yellow) and a few noncentrosomal (cyan) tracks in the cell center and their relation to the Golgi position.

(G) No alteration of centrosomal MT tracks upon CLASP (CLkd, blue) or GCC185 (GCCkd, green) knockdown. Error bars indicate standard deviations.

(H) Decrease in Golgi-associated MT track number upon CLASP (CLkd, blue) or GCC185 (GCCkd, green) knockdown. Error bars indicate standard deviations.
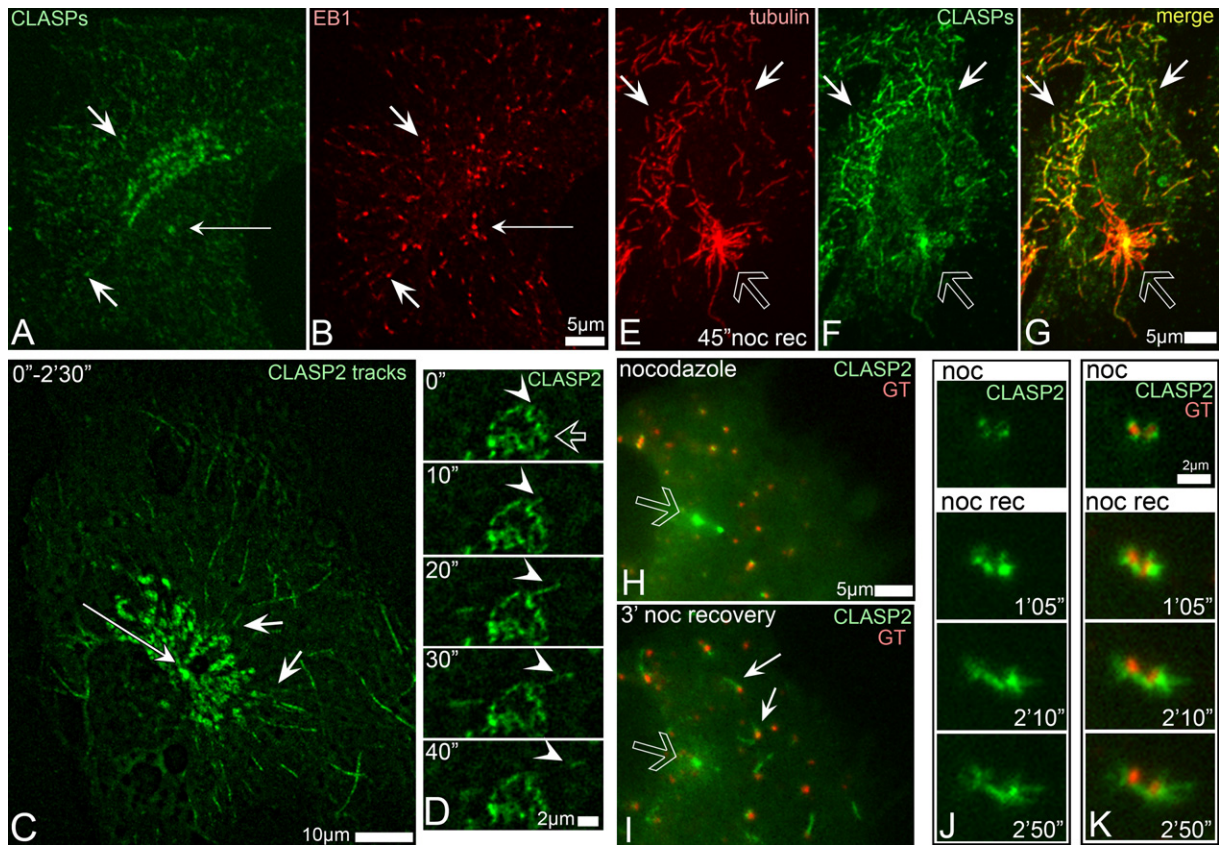
**Figure 6. CLASPs Preferentially Bind to MTs Originated at the Golgi**

(A) CLASPs (green) in RPE1 cells are associated with MT tips close to the Golgi (short arrows), but not around the centrosome (thin arrow).

(B) EB1 (red) at the MT tips in the cell shown in (A). Immunostaining.

(C) Overlaid live recording of GFP-CLASP2-expressing RPE1 cell within 2.5 min. CLASP2-associated MT tracks (short arrows) radiate from the TGN but not from the centrosome (thin arrow).

(D) Live sequence illustrating formation of a GFP-CLASP2-decorated MT (arrowhead) at the CLASP-rich TGN (hollow arrow) in an untreated cell. CLASP2 coats whole newly formed MTs (10–20 s) but remains only at the tip at a later stage (30–40 s).

(E–G) A cell fixed 45 s after nocodazole washout. (E) Tubulin (red). (F) CLASPs (green). (G) Merge. CLASPs localize to noncentrosomal (white arrows) but not to centrosomal (hollow arrow) MTs.

(H and I) GFP-CLASP2 (green) localizations before and after nocodazole washout. In nocodazole (H), CLASP2 associates with Golgi stacks (mCherry-GT, red) and with the centrosome (hollow arrow). Three minutes after nocodazole removal (I), CLASP2 is detected at the Golgi-associated MTs (white arrows) but not around the centrosome (hollow arrow).

(J and K) Video frames illustrating formation of GFP-CLASP2-coated MTs at GFP-CLASP2-enriched Golgi stacks in nocodazole washout. (J) GFP-CLASP2. (K) GFP-CLASP2, green; mCherry-GT, red. Time after nocodazole removal is shown.

72 hr after transfection, as at this time minimal protein levels were detected. siRNA oligos against $\gamma$-tubulin were transfected two times within 72 hr as described in Luders et al. (2006). Anti-GCC185 siRNA oligos (corresponding to nucleotides 767–784 in KIAA0336 cDNA) were designed by Ambion. GCC185 from myc-GCC185 was cloned into XhoI/BamHI restriction sites of a Venus-C1 vector (J. Roland, modified from Clontech). A rescue construct was made by site-directed mutagenesis to substitute six nucleotides in an area recognized by siRNA (siRNA targeted sequence: 5′-G GCT AAT TCT CAG CAT TAC C-3′; mutant sequence: 5′-G GCC AAC TCC CAA CAC TAT C-3′). Nontargeting siRNA (Dharmacon) was used for controls. mCherry plasmid used for red fluorescent imaging was kindly provided by Dr. R. Tsien (San Diego). YFP-GT (YFP-Golgi marker; Clontech) and mCherry-GT (modified from Clontech) were used for Golgi visualization. EGFP-EB3 and mCherry-EB3 (kind gift of Dr. J.V. Small, Vienna), mCherry-tubulin (kind gift of Dr. R. Tsien, San Diego), and 3GFP-EMTB (kind gift of Dr. J.C. Bulinski, New York) were used for MT plus tip and MT visualization. GFP-centrin (kind gift of Dr. M. Bornens, Paris) was used for centrosome visualization in laser ablation experiments. GFP-CLASP1α, GFP-CLASP2α, and the nonsilenceable rescue construct GFP-CLASP2 are described in Mimori-Kiyosue et al. (2005). Myc-tagged GCC185 construct is described in Luke et al. (2003). mCherry-dTOM20 (*Drosophila* outer mitochondrial protein) was kindly provided by Dr. E. Lee (Nashville). Mito-CLASP (dTOM20 fused with the N-terminal end of CLASP2α in a pCS2 vector) was used for CLASP mislocalization to mitochondria. Transient transfections were

(I and J) CLASPs (I) and MTs (J) in mixed culture of CLASP-positive (white arrows) and CLASP-depleted (hollow arrows) cells.

(K and L) GCC185 (K) and MTs (L) in mixed culture of control (white arrows) and GCC185-depleted (hollow arrows) cells. CLASP- or GCC185-depleted cells lack a Golgi-associated MT array. Immunostaining.
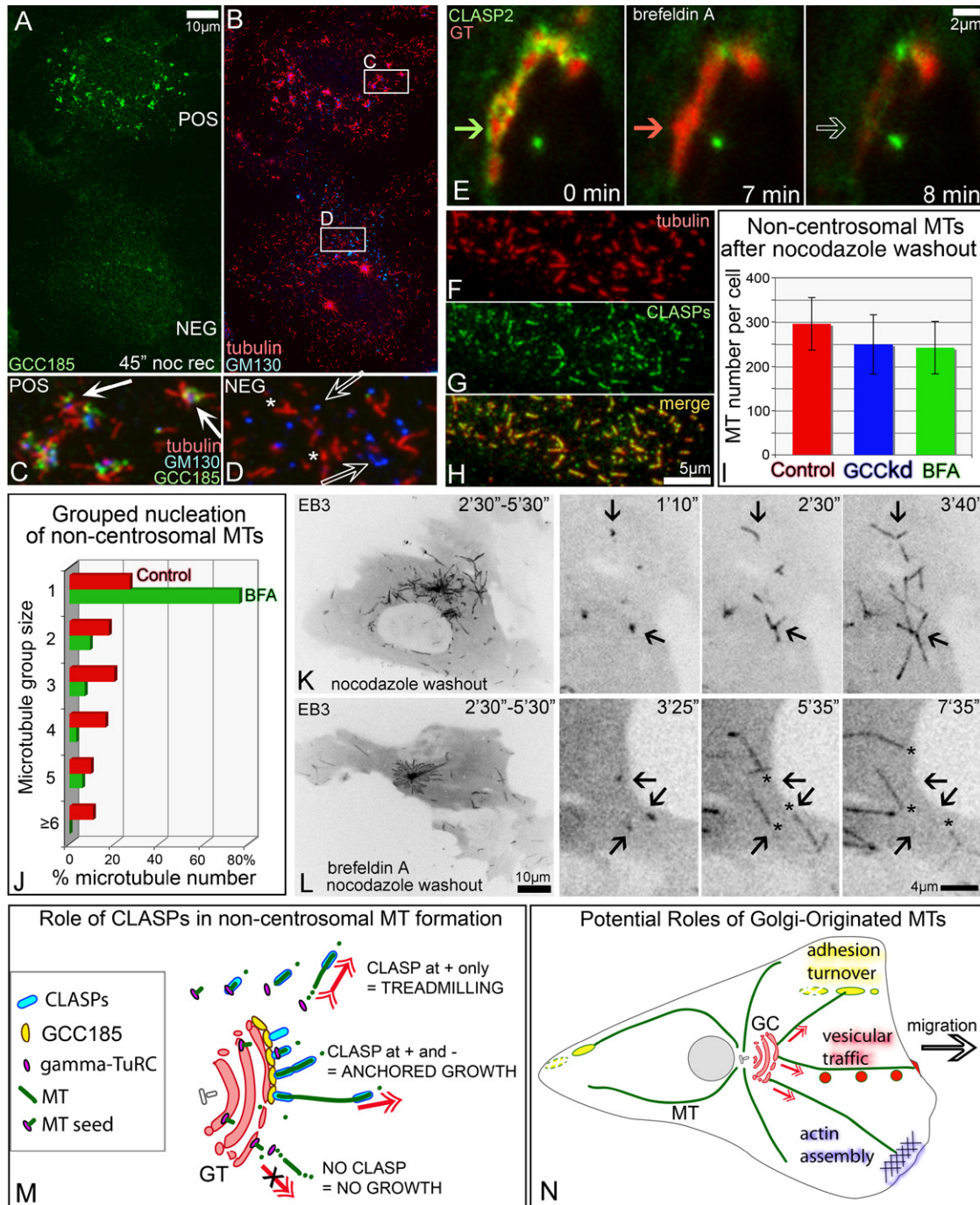
**Figure 7. CLASPs Dissolved in the Cytosol Support MT Nucleation but Not Minus End Anchoring**

(A–D) Mixed culture of GCC185-positive (pos) and GCC185-depleted (neg) cells 45 s after nocodazole washout. Boxes from (B) are enlarged in (C) and (D). GCC185, green (A, C, and D); tubulin, red (B–D); GM130, blue (B–D). (C) In a control cell, MTs grow from the Golgi stacks. (D) In GCC185-depleted cells, Golgi stacks (hollow arrows) are not associated with random single MTs (asterisks).

(E) In brefeldin A, GFP-CLASP2 (green) dissociates from the Golgi (7 min) prior to Golgi-ER fusion (8 min). Fusion is visualized by acute loss of mCherry-GT signal (red). Arrow hue illustrates presence of proteins. Time in brefeldin A is shown.

(F–H) In brefeldin A, CLASPs coat noncentrosomal MTs formed 45 s after nocodazole washout. (F) Tubulin. (G) CLASPs. (H) Merge. Immunostaining.

(I) MTs formed in control (red), GCC185-depleted (GCCkd; blue), and brefeldin A-treated (BFA; green) cells 45 s after nocodazole washout. For each set, 30 cells immunostained for tubulin were analyzed. Error bars indicate standard deviations.

(J) Number of MTs nucleated singly and in groups after nocodazole washout with (BFA; green) and without (red) brefeldin A. Live recordings of seven mCherry-EB3-expressing cells for each set were analyzed.

performed with Fugene6 (Roche) according to the manufacturer's protocol.

### Antibodies

For rabbit polyclonal antibodies against CLASP2 VU-83, see Supplemental Data and Figure S3. For guinea pig polyclonal antibodies against GCC185 VU-140, see Supplemental Data and Figure S9. Rabbit polyclonal antibodies against CLASP2 are described in Akhmanova et al. (2001). Rabbit polyclonal antibodies against CLIP170 are described in Coquelle et al. (2002). Rabbit polyclonal antibodies against CLASP1 were kindly provided by Dr. F. Severin (Dresden). For Golgi compartment identification, a mouse monoclonal antibody against GM130 (Transduction Laboratories) and a rabbit polyclonal antibody against GCC185 (Luke et al., 2003) were used. Myc tag was identified by monoclonal anti-myc antibody clone 9E10 (Upstate). Mouse monoclonal antibodies against EB1 and p150 Glued were from Transduction Laboratories, a rat monoclonal antibody against Tyr-tubulin was from Abcam, and anti-$\alpha$-tubulin and anti-$\gamma$-tubulin mouse monoclonal and rabbit polyclonal antibodies were from Sigma.

### Immunofluorescence, Confocal, and Live-Cell Imaging

Wide-field fluorescence imaging was performed using a Nikon 80I microscope with a CFI APO 60× oil lens, NA 1.4, and a CoolSnap ES CCD camera (Photometrics).

Confocal stacks were taken by a Yokogawa QLC-100/CSU-10 spinning disk head (Visitec assembled by Vashaw) attached to a Nikon TE2000E microscope using a CFI PLAN APO VC 100× oil lens, NA 1.4, with or without 1.5× intermediate magnification, and a back-illuminated EM-CCD camera Cascade 512B (Photometrics) driven by IPLab software (Scanalytics). A krypton-argon laser (75 mW 488/568; Melles Griot) with AOTF was used for two-color excitation. Custom double dichroic mirror and filters (Chroma) in a filter wheel (Ludl) were used in the emission light path. Z steps (0.2 $\mu$m) were driven by a Nikon built-in Z motor.

Live cells plated on MatTech glass bottom dishes were maintained at 37°C by heated stage (Warner Instruments) on a Nikon TE2000E inverted microscope equipped with a PerfectFocus automated focusing device. Single-plane confocal video sequences were taken as described for confocal stacks. A similar setup with a Pinkel triple-filter set (Semrock) was used for nearly simultaneous two-color wide-field imaging.

For image-processing details, see Supplemental Data.

### Centrosome Ablation

Centrosome ablation was carried out as described elsewhere (Khodjakov et al., 2000; La Terra et al., 2005). Briefly, 532 nm 8 ns laser pulses generated by a Q-switched Nd:YAG laser (Diva II; Thales Lasers) were focused on the specimen with a 100× 1.4 NA PlanApo lens.

Centrosomes were identified via centrin-GFP expression and ablated with approximately 10–20 laser pulses (0.5–1.0 s). Fluorescence images were recorded with a back-illuminated EM-CCD camera (Cascade 512B; Photometrics) in confocal mode (spinning disk confocal; Perkin-Elmer). All light sources were shuttered by either fast mechanical shutters (Vincent Associates) or AOTF (Solamere Technology Group), so that cells were exposed to light only during laser operations and/or image acquisition.

### Coimmunoprecipitation, LAP Tagging, and Mass Spectrometry

HEK293T cells transiently transfected with myc-GCC185 were used for immunoprecipitation with affinity-purified anti-CLASP antibody VU-83 or anti-myc monoclonal antibody 9E10. The precipitated protein complexes were analyzed by western blotting. HeLa cells stably expressing the GFP-CLASP1$\alpha$ (LAP) construct in the pIC113 vector were used for GFP-CLASP1 (LAP) fusion immunoprecipitation by anti-GFP antibodies as described (Cheeseman and Desai, 2005). TEV protease-cleaved CLASP protein was desalted and analyzed using a modified 12-step separation described previously (Washburn et al., 2001). MS/MS spectra were searched with the SEQUEST algorithm (Eng et al., 1994). Several steps of filtering were applied. Usual contaminants obtained by this technique were excluded from possible CLASP1 interactors. See Supplemental Data for protocol details.

### Supplemental Data

Supplemental Data include nine figures, one table, nine movies, and Supplemental Experimental Procedures and are available at http://www.developmentalcell.com/cgi/content/full/12/6/917/DC1/.

### REFERENCES

Akhmanova, A., Hoogenraad, C.C., Drabek, K., Stepanova, T., Dortland, B., Verkerk, T., Vermeulen, W., Burgering, B.M., De Zeeuw, C.I., Grosveld, F., and Galjart, N. (2001). CLASPs are CLIP-115 and -170 associating proteins involved in the regional regulation of microtubule dynamics in motile fibroblasts. Cell *104*, 923–935.

Bacallao, R., Antony, C., Dotti, C., Karsenti, E., Stelzer, E.H., and Simons, K. (1989). The subcellular organization of Madin-Darby canine kidney cells during the formation of a polarized epithelium. J. Cell Biol. *109*, 2817–2832.

Bartolini, F., and Gundersen, G.G. (2006). Generation of noncentrosomal microtubule arrays. J. Cell Sci. *119*, 4155–4163.

Bergen, L.G., Kuriyama, R., and Borisy, G.G. (1980). Polarity of microtubules nucleated by centrosomes and chromosomes of Chinese hamster ovary cells in vitro. J. Cell Biol. *84*, 151–159.

Bugnard, E., Zaal, K.J., and Ralston, E. (2005). Reorganization of microtubule nucleation during muscle differentiation. Cell Motil. Cytoskeleton *60*, 1–13.

---

(K and L) Noncentrosomal MTs in GFP-EB3-expressing RPE1 cells. Inverted images. Left, EB3 tracks within 3′. Right, enlarged inset video frames. Time after nocodazole removal is shown. (K) In a control cell, MTs grow from distinct centers (arrows). (L) In brefeldin A-treated cells, minus ends of single MTs (asterisks) do not remain at the nucleation sites (arrows).

(M) Model for mechanisms of CLASP-dependent MT formation. $\gamma$-tubulin nucleates MT seeds in cytosol or at the Golgi. Cytoplasmic CLASPs associate with the MT plus end and support polymerization whereas the minus end is unstable and depolymerizes, resulting in MT treadmilling (top). CLASPs bound to the TGN via GCC185 coat the MT portion proximal to the minus end, anchor it to the membrane, and prevent its depolymerization, while the CLASP-associated plus end steadily grows (middle). In the absence of CLASPs, MT seeds are unstable (bottom).

(N) Potential roles of Golgi-originated MTs in cell migration (model). Front-oriented MTs likely support post-Golgi vesicular trafficking (red), actin polymerization (blue), and focal adhesion turnover behind the leading edge (yellow). GC, Golgi complex.

Chabin-Brion, K., Marceiller, J., Perez, F., Settegrana, C., Drechou, A., Durand, G., and Pous, C. (2001). The Golgi complex is a microtubule-organizing organelle. Mol. Biol. Cell *12*, 2047–2060.

Cheeseman, I.M., and Desai, A. (2005). A combined approach for the localization and tandem affinity purification of protein complexes from metazoans. Sci. STKE *2005*, pl1.

Coquelle, F.M., Caspi, M., Cordelieres, F.P., Dompierre, J.P., Dujardin, D.L., Koifman, C., Martin, P., Hoogenraad, C.C., Akhmanova, A., Galjart, N., et al. (2002). LIS1, CLIP-170's key to the dynein/dynactin pathway. Mol. Cell. Biol. *22*, 3089–3102.

de Anda, F.C., Pollarolo, G., Da Silva, J.S., Camoletto, P.G., Feiguin, F., and Dotti, C.G. (2005). Centrosome localization determines neuronal polarity. Nature *436*, 704–708.

Drabek, K., van Ham, M., Stepanova, T., Draegestein, K., van Horssen, R., Sayas, C.L., Akhmanova, A., Ten Hagen, T., Smits, R., Fodde, R., et al. (2006). Role of CLASP2 in microtubule stabilization and the regulation of persistent motility. Curr. Biol. *16*, 2259–2264.

Eng, J., McCormack, A., and Yates, J. (1994). An approach to correlate tandem mass spectral data of peptides with amino acid sequences in a protein database. J. Am. Soc. Mass Spectrom. *5*, 976–989.

Higginbotham, H., Tanaka, T., Brinkman, B.C., and Gleeson, J.G. (2006). GSK3β and PKCζ function in centrosome localization and process stabilization during Slit-mediated neuronal repolarization. Mol. Cell. Neurosci. *32*, 118–132.

Khodjakov, A., and Rieder, C.L. (2001). Centrosomes enhance the fidelity of cytokinesis in vertebrates and are required for cell cycle progression. J. Cell Biol. *153*, 237–242.

Khodjakov, A., Cole, R.W., Oakley, B.R., and Rieder, C.L. (2000). Centrosome-independent mitotic spindle formation in vertebrates. Curr. Biol. *10*, 59–67.

Komarova, Y.A., Vorobjev, I.A., and Borisy, G.G. (2002). Life cycle of MTs: persistent growth in the cell interior, asymmetric transition frequencies and effects of the cell boundary. J. Cell Sci. *115*, 3527–3539.

Ladinsky, M.S., Wu, C.C., McIntosh, S., McIntosh, J.R., and Howell, K.E. (2002). Structure of the Golgi and distribution of reporter molecules at 20°C reveals the complexity of the exit compartments. Mol. Biol. Cell *13*, 2810–2825.

Lansbergen, G., Grigoriev, I., Mimori-Kiyosue, Y., Ohtsuka, T., Higa, S., Kitajima, I., Demmers, J., Galjart, N., Houtsmuller, A.B., Grosveld, F., and Akhmanova, A. (2006). CLASPs attach microtubule plus ends to the cell cortex through a complex with LL5β. Dev. Cell *11*, 21–32.

La Terra, S., English, C.N., Hergert, P., McEwen, B.F., Sluder, G., and Khodjakov, A. (2005). The de novo centriole assembly pathway in HeLa cells: cell cycle progression and centriole assembly/maturation. J. Cell Biol. *168*, 713–722.

Luders, J., Patel, U.K., and Stearns, T. (2006). GCP-WD is a γ-tubulin targeting factor required for centrosomal and chromatin-mediated microtubule nucleation. Nat. Cell Biol. *8*, 137–147.

Luke, M.R., Kjer-Nielsen, L., Brown, D.L., Stow, J.L., and Gleeson, P.A. (2003). GRIP domain-mediated targeting of two new coiled-coil proteins, GCC88 and GCC185, to subcompartments of the *trans*-Golgi network. J. Biol. Chem. *278*, 4216–4226.

Malikov, V., Kashina, A., and Rodionov, V. (2004). Cytoplasmic dynein nucleates microtubules to organize them into radial arrays in vivo. Mol. Biol. Cell *15*, 2742–2749.

Mimori-Kiyosue, Y., Grigoriev, I., Lansbergen, G., Sasaki, H., Matsui, C., Severin, F., Galjart, N., Grosveld, F., Vorobjev, I., Tsukita, S., and

Akhmanova, A. (2005). CLASP1 and CLASP2 bind to EB1 and regulate microtubule plus-end dynamics at the cell cortex. J. Cell Biol. *168*, 141–153.

Mironov, A.A., Beznoussenko, G.V., Polishchuk, R.S., and Trucco, A. (2005). Intra-Golgi transport: a way to a new paradigm? Biochim. Biophys. Acta *1744*, 340–350.

Musch, A. (2004). Microtubule organization and function in epithelial cells. Traffic *5*, 1–9.

Piehl, M., Tulu, U.S., Wadsworth, P., and Cassimeris, L. (2004). Centrosome maturation: measurement of microtubule nucleation throughout the cell cycle by using GFP-tagged EB1. Proc. Natl. Acad. Sci. USA *101*, 1584–1588.

Preisinger, C., Short, B., De Corte, V., Bruyneel, E., Haas, A., Kopajtich, R., Gettemans, J., and Barr, F.A. (2004). YSK1 is activated by the Golgi matrix protein GM130 and plays a role in cell migration through its substrate 14-3-3ζ. J. Cell Biol. *164*, 1009–1020.

Presley, J.F., Smith, C., Hirschberg, K., Miller, C., Cole, N.B., Zaal, K.J., and Lippincott-Schwartz, J. (1998). Golgi membrane dynamics. Mol. Biol. Cell *9*, 1617–1626.

Prigozhina, N.L., and Waterman-Storer, C.M. (2004). Protein kinase D-mediated anterograde membrane trafficking is required for fibroblast motility. Curr. Biol. *14*, 88–98.

Raftopoulou, M., and Hall, A. (2004). Cell migration: Rho GTPases lead the way. Dev. Biol. *265*, 23–32.

Reilein, A., and Nelson, W.J. (2005). APC is a component of an organizing template for cortical microtubule networks. Nat. Cell Biol. *7*, 463–473.

Rid, R., Schiefermeier, N., Grigoriev, I., Small, J.V., and Kaverina, I. (2005). The last but not the least: the origin and significance of trailing adhesions in fibroblastic cells. Cell Motil. Cytoskeleton *61*, 161–171.

Rios, R.M., Sanchis, A., Tassin, A.M., Fedriani, C., and Bornens, M. (2004). GMAP-210 recruits γ-tubulin complexes to *cis*-Golgi membranes and is required for Golgi ribbon formation. Cell *118*, 323–335.

Salaycik, K.J., Fagerstrom, C.J., Murthy, K., Tulu, U.S., and Wadsworth, P. (2005). Quantification of microtubule nucleation, growth and dynamics in wound-edge cells. J. Cell Sci. *118*, 4113–4122.

Shanks, R.A., Steadman, B.T., Schmidt, P.H., and Goldenring, J.R. (2002). AKAP350 at the Golgi apparatus. I. Identification of a distinct Golgi apparatus targeting motif in AKAP350. J. Biol. Chem. *277*, 40967–40972.

Suter, D.M., Schaefer, A.W., and Forscher, P. (2004). Microtubule dynamics are necessary for SRC family kinase-dependent growth cone steering. Curr. Biol. *14*, 1194–1199.

Washburn, M.P., Wolters, D., and Yates, J.R., III. (2001). Large-scale analysis of the yeast proteome by multidimensional protein identification technology. Nat. Biotechnol. *19*, 242–247.

Waterman-Storer, C.M., Worthylake, R.A., Liu, B.P., Burridge, K., and Salmon, E.D. (1999). Microtubule growth activates Rac1 to promote lamellipodial protrusion in fibroblasts. Nat. Cell Biol. *1*, 45–50.

Wittmann, T., and Waterman-Storer, C.M. (2005). Spatial regulation of CLASP affinity for microtubules by Rac1 and GSK3β in migrating epithelial cells. J. Cell Biol. *169*, 929–939.

Yvon, A.M., and Wadsworth, P. (1997). Non-centrosomal microtubule formation and measurement of minus end microtubule dynamics in A498 cells. J. Cell Sci. *110*, 2391–2401.